Table 4. Differences in the mean number of symptoms within the patient group and between the two groups dichotomized at the limit of quantification of serum VOCs.

Compound	Mean No. of symptoms		*p* Value
	Serum VOC positive	Serum VOC negative	
p-Dichlorobenzene	5.5	7.0	0.3187
Toluene	7.5	5.0	0.0701
Xylene	6.0	6.2	0.8906

Table 4 shows a summary of the mean number of symptoms within the patient group. The differences in the number of symptoms are not statistically significant between the two groups dichotomized at the limit of quantification of serum VOCs.

These results indicate that it is difficult to determine the serum VOC levels responsible for inducing symptoms.

Several reports have suggested that SBS symptoms are related to VOCs in the indoor air environment (Norbäck et al. 2000; Kamijima et al. 2002; Saijo et al. 2004); however, there has been no report on the relationship between serum VOC levels and SBS symptoms to our certain knowledge. In this study we measured serum levels of VOCs in patients with SBS symptoms and volunteer controls. Measuring chemicals in blood is advantageous because we can calculate the body burden precisely. However, for nonoccupationally exposed people, it is generally difficult to clarify the relationship between adverse effects and VOC exposure or serum VOC levels because of the relatively low levels of VOCs found in serum (Ashley et al. 1994). The serum VOC levels of all subjects in this study were relatively low except for *p*-dichlorobenzene, which was consistent with previous reports (Ashley et al. 1996). The number of target VOCs was limited although there are more than one hundred VOCs in indoor air. The small subject population restricted our approach to include limited statistical analysis. Detailed information on the patients' history of exposure is lacking. Further investigation to overcome these problems is required.

In this study we intended to examine (1) whether HS-GC/MS was applicable to the measurement of serum VOC concentrations in SBS patients and volunteer controls, and (2) whether the elevation of serum VOC levels correlated with SBS symptoms. Despite the successful application of our HS-GC/MS method, we found no statistical differences in the concentrations of studied VOCs between the patients and controls. We also found no relationship between serum VOC levels and SBS symptoms in the patients studied. Therefore, we must consider that it is difficult to identify the responsible VOCs and their serum levels inducing SBS symptoms from the results of this study.

Acknowledgments This study was supported by Health Sciences Research grants from the Ministry of Health, Labor and Welfare of Japan.

REFERENCES

Ashley DL, Bonin MA, Cardinali FL, McCraw JM, Wooten JV (1994) Blood

concentrations of volatile organic compounds in a nonoccupationally exposed US population and in groups with suspected exposure. Clin Chem 40: 1401-1404.

Ashley DL, Bonin MA, Cardinali FL, McCraw JM, Wooten JV (1996) Measurement of volatile organic compounds in human blood. Environ Health Perspect 104: 871-877.

Hodgson M (2002) Indoor environmental exposures and symptoms. Environ Health Perspect 110: 663-667.

Kamijima M, Sakai K, Shibata E, Yamada T, Itohara S, Ohno H, Hayakawa R, Sugiura M, Yamaki K, Takeuchi Y (2002) 2-Ethyl-1-hexanol in indoor air as a possible cause of sick building symptoms. J Occup Health 44: 186-191.

Mannino D, Schreiber J, Aldous K, Ashley D, Moolenaar R, Almaguer D (1995) Human exposure to volatile organic compounds: a comparison of organic vapor monitoring badge levels with blood levels. Int Arch Occup Environ Health 67: 59-64.

Norbäck D, Wieslander G, Nordström K, Wålinder R (2000) Asthma symptoms in relation to measured building dampness in upper concrete floor construction, and 2-ethyl-1-hexanol in indoor air. Int J Tuberc Lung Dis 4: 1016-1025.

Redlich CA, Sparer J, Cullen MR (1997) Sick-building syndrome. Lancet 349: 1013-1016.

Stenberg B, Wall S (1995) Why do women report 'sick building symptoms' more often than men? Soc Sci Med 40: 491-502.

Saijo Y, Kishi R, Sata F, Katakura Y, Urashima Y, Hatakeyama A, Kobayashi S, Jin K, Kurahashi N, Kondo T, Gong YY, Umemura T (2004) Symptoms in relation to chemicals and dampness in newly built dwellings. Int Arch Occup Environ Health 77: 461-470.

STEM CELLS
STEM CELL GENETICS AND GENOMICS

Dimethyl Sulfoxide Has an Impact on Epigenetic Profile in Mouse Embryoid Body

MISA IWATANI, KOHTA IKEGAMI, YULIYA KREMENSKA, NAKA HATTORI, SATOSHI TANAKA, SHINTARO YAGI, KUNIO SHIOTA

Laboratory of Cellular Biochemistry, Department of Animal Resource Sciences/Veterinary Medical Sciences, The University of Tokyo, Tokyo, Japan

Key Words. Dimethyl sulfoxide • DNA methylation • Epigenetics • Differentiation • DNA methyltransferase

ABSTRACT

Dimethyl sulfoxide (DMSO), an amphipathic molecule, is widely used not only as a solvent for water-insoluble substances but also as a cryopreservant for various types of cells. Exposure to DMSO sometimes causes unexpected changes in cell fates. Because mammalian development and cellular differentiation are controlled epigenetically by DNA methylation and histone modifications, DMSO likely affects the epigenetic system. The effects of DMSO on transcription of three major DNA methyltransferases (Dnmts) and five well-studied histone modification enzymes were examined in mouse embryonic stem cells and embryoid bodies (EBs) by reverse transcription-polymerase chain reaction. Addition of DMSO (0.02%–1.0%) to EBs in culture induced an increase in Dnmt3a mRNA levels with increasing dosage. Increased expression of two subtypes of Dnmt3a in protein levels was confirmed by Western blotting. Southern blot analysis revealed that DMSO caused hypermethylation of two kinds of repetitive sequences in EBs. Furthermore, restriction landmark genomic scanning, by which DNA methylation status can be analyzed on thousands of loci in genic regions, revealed that DMSO affected DNA methylation status at multiple loci, inducing hypomethylation as well as hypermethylation depending on the genomic loci. In conclusion, DMSO has an impact on the epigenetic profile: upregulation of Dnmt3a expression and alteration of genome-wide DNA methylation profiles with phenotypic changes in EBs. STEM CELLS *2006;24:2549–2556*

INTRODUCTION

Dimethyl sulfoxide (DMSO), an amphipathic molecule, is one of the most commonly used chemicals in the biological and medical sciences as a solvent for water-insoluble substances and a cryopreservant for various cell lines. It has multiple effects on cellular functions (e.g., metabolism and enzymatic activity) and on cell growth by affecting cell cycle and apoptosis [1]. It also changes cell fates by inducing differentiation of various types of cells [1–4] and promoting blastocyst formation in animal cloning [5].

Mammalian development and cellular differentiation are controlled by DNA methylation; the developmentally essential genes *Oct-4* and *Sry* are controlled to be expressed during a limited period of development by DNA methylation [6, 7]. Methylation is the sole modification of the vertebrate genome and occurs mainly at the 5-position of cytosines in cytosine-guanine (CpG) dinucleotides [8]. The modification is involved in epigenetic regulation of gene function, which is "mitotically and/or meiotically heritable, and can not be explained by changes in DNA sequences" [9]. Epigenetic systems regulate various genetic functions, including chromosomal stability, repression of transposable elements, and gene silencing [10–12] of developmentally regulated genes and genes expressed in a tissue-specific manner [13, 14]. Tissue-dependent and differentially methylated regions (T-DMRs) have been found in CpG-rich, unique sequences, including tissue-specific genes. The changes in genome-wide DNA methylation status of such T-DMRs provide every cell or tissue a unique DNA methylation profile consisting of methylated and unmethylated T-DMRs [15–17].

In the establishment and maintenance of the proper DNA methylation patterns in the mammalian genome, DNA methyltransferases (Dnmts) play critical roles. To date, five Dnmts, Dnmt1, 2, 3a, 3b, and 3L, have been identified. Because in vitro enzymatic activity is lacking in Dnmt2 and 3L [18, 19], only Dnmt1, Dnmt3a, and Dnmt3b have been intensively studied [20,

Correspondence: Kunio Shiota, D.V.M., Ph.D., Laboratory of Cellular Biochemistry, Department of Animal Resource Sciences/Veterinary Medical Sciences, The University of Tokyo, 1-1-1 Yayoi, Bunkyo-ku, Tokyo, 113-8657, Japan. Telephone: +81-3-5841-5472; Fax: +81-3-5841-8189; e-mail: ashiota@mail.ecc.u-tokyo.ac.jp Received August 31, 2005; accepted for publication July 1, 2006; first published online in STEM CELLS *EXPRESS* July 13, 2006. 1066-5099/2006/$20.00/0 doi: 10.1634/stemcells.2005-0427

21]. DNA methylation is associated with histone modifications in epigenetically regulated regions [20, 22–24]. Histone modifications were mediated by the following enzymes: G9a, Suv39h1, and Suv39h2 are histone H3 lysine nine (H3-K9) methyltransferases [12]; mDot1 is an H3-K79 methyltransferase [25]; and Sir2α is a class III histone deacetylase [26]. These enzymes and Dnmts coordinate the epigenetic systems.

Mutations in genes of epigenetic factors have been implicated as the causes of various diseases. Mutations in DNMT3b are associated with ICF syndrome (immunodeficiency, centromere instability, and facial abnormalities) [27], and those in MeCP2 are associated with Rett syndrome [28]. Epigenetic abnormalities have been reported in cloned animals [29–31] and cancerous cells [32] and are also caused by chemicals that are called "epimutagens" [33].

Based on these observations, we hypothesized that the effects on cell fate by DMSO should be interpreted by its effects on the epigenetic systems. We examined this hypothesis by using mouse embryonic stem cells (ESCs) and embryoid bodies (EBs). Differentiation of ESCs into EBs has been used as a model of normal and abnormal mammalian development [34]. It is also a suitable model for monitoring epigenetic modifications because, during differentiation from ESCs, EBs establish a specific DNA methylation profile associated with both hypermethylation and hypomethylation at multiple loci [16]. In this study, mRNA levels of epigenetic regulators, including Dnmts and histone modification enzymes, were analyzed. We also investigated a genome-wide DNA methylation profile in EBs to examine the effects of quantitative changes in an enzyme's expression.

Materials and Methods

Culture of ESCs, EBs, and DMSO Treatment

The ESC lines (MS12) derived from C57BL/6 strain mice [35] were cultured on embryonic fibroblast feeder cells with ESC medium: Dulbecco's modified Eagle's medium (DMEM; Invitrogen, Carlsbad, CA, http://www.invitrogen.com) supplemented with 15% fetal bovine serum and 1,000 U/ml of leukemia inhibitory factor (LIF; ESGRO, Chemicon International, Temecula, CA, http://www.chemicon.com). At passage 18, ESCs were treated with or without 0.1% (vol/vol) DMSO (Wako Pure Chemicals, Osaka, Japan, http://www.wako-chem.co.jp/english) for 4 days and harvested. EBs were induced by culturing ESCs at passage 16 without a feeder layer and LIF in bacteriological Petri dishes and simultaneously treated with or without DMSO. They were cultured under DMSO treatment for 4 days in EB medium:DMEM (Invitrogen) supplemented with 10% fetal bovine serum and then collected for nucleic acids and protein extractions.

RNA Extraction and Reverse Transcription-Polymerase Chain Reaction

Total RNA was purified from cultured ESCs and EBs using TRIzol reagent (Invitrogen) according to the manufacturer's instructions. For reverse transcription-polymerase chain reaction (RT-PCR), first-strand cDNA was synthesized from 1.0 μg of total RNA using a Superscript first-strand synthesis system with random hexamer primers (Invitrogen). RT-PCR was performed with rTaq polymerase (TOYOBO, Tokyo, http://www.toyobo.co.jp/e) except in the case of Dnmt3a, which was amplified with Immolase (BIOLINE, London, http://www.bioline.com). Sets of primer sequences for RT-PCR were as follows: Dnmt1: 5′-CAGGAGTGTGTGAGGGAG-3′ and 5′-GGTGTCACTGTCCGACTTGC-3′, Dnmt3a: 5′-ACCCATGCCAAGACTCACCTTC-3′ and 5′-TCCACCTTCTGAGACTCTCCAG-3′, Dnmt3b: 5′-TCAGACACGAAGGATGCTCC-3′ and 5′-ACAGGGTACTCCTGCACATG-3′, G9a: 5′-TTTGGCCATGAGGCTGTT-3′ and 5′-CCAGATGCATGTCATCACTCA-3′, Suv39h1: 5′-GGAGAAAGATGGCGGAAA-3′ and 5′-GACAAGAAAGCTTGGCTAGT-3′, Suv39h2: 5′-TCTTTGGCGACGAGTGTG-3′ and 5′-AGAATCTGGCCATCCTTTCC-3′, Sir2α: 5′-CTGACGACTTCGACGACGAC-3′ and 5′-TGCTGAACAAAAGTATATGGACCTATC-3′, mDot1: 5′-AACTATGTCCTGATCGACTACG-3′ and 5′-TCCTCTGTCATCTTGATCTCATC-3′, and β-actin: 5′-TTCTACAATGAGCTGCGTGTGG-3′ and 5′-ATGGCTGGGGTGTTGAAGGT-3′. The thermocycling program used with rTaq polymerase was an initial cycle of 95°C for 1 minute, followed by 30 cycles of 94°C for 30 seconds, and 30 seconds at the following annealing temperatures: 58°C for β-actin, 60°C for Suv39h1, 62°C for Dnmt1 and mDot1, and 65°C for Dnmt3b, G9a, Suv39h2, and Sir2α and then 72°C for 1 minute. RT-PCR for Dnmt3a using Immolase was performed with an initial cycle of 95°C for 10 minutes, followed by 30 cycles of 94°C for 30 seconds, 65°C for 30 seconds, and 72°C for 1 minute. A digitized image of ethidium bromide-stained gel was analyzed by densitometry with NIH Image 1.61 software (National Institutes of Health, Bethesda, MD, http://www.nih.gov).

Real-Time Quantitative RT-PCR

Expression of Dnmt3a was monitored by SYBR Green I in SYBR Green PCR Master Mix (Applied Biosystems, Foster City, CA, http://www.appliedbiosystems.com) on a ABI PRISM 7500 or 7900 HT sequence detection system (Applied Biosystems) according to the manufacturer's protocol. Nine nanomolar each of forward and reverse primers described above for Dnmt3a or β-actin and 1 μl and 0.5 μl of cDNAs were used for Dnmt3a and β-actin, respectively, in 20 μl. A standard curve was established by a dilution series of cDNA to estimate mRNA levels. Correlation values (r^2) of the standard curve were 0.98 and 0.99 for Dnm3a and β-actin, respectively. The slope of the standard curve was determined to calculate PCR efficiency using the equation: PCR efficiency = $10^{-1/\text{slope}} - 1$. The values for Dnmt3a and β-actin were 1.04 and 1.00, respectively. Quantitative expression level was calculated using the following equation: the value = $1/(1 + \text{PCR efficiency})^{CT}$. The slope of the standard curve and cycle thresholds (CTs) were analyzed using ABI PRISM 7500 SDS software. Expression of Dnmt3a was normalized to β-actin as an internal control. At least three independent PCRs were performed in duplicate for all samples.

Protein Extraction and Western Blotting

Mouse EBs and ESCs were lysed in RIPA buffer (50 mM Tris-HCl [pH 8.0], 400 mM NaCl, 1% Nonident P-40, 1% sodium deoxycholate, 0.1% SDS, 1 mM phenylmethylsulfonyl fluoride, 5 μg/ml leupeptin, 1 μg/ml aprotinin, 5 μg/ml pepstatin, 0.5 mM EDTA, and 0.5 mM NaF). The lysates were clarified by centrifugation at 15,000 rpm for 30 minutes at 4°C, and 5-μg aliquots of the lysates were subjected to SDS polyacrylamide gel electrophoresis on 7.5%

gel. Protein concentration was determined by using a bicinchoninic acid protein assay kit (Pierce Chemical, Rockford, IL, http://www.piercenet.com) according to the manufacturer's instructions. The proteins were transferred to polyvinylidene difluoride membrane and probed with 1:125 diluted anti-Dnmt3a monoclonal antibody (clone 64B1446; Imgenex, San Diego, http://www.Imgenex.com) or 1:1,000 diluted anti-glyceraldehyde-3-phosphate dehydrogenase monoclonal antibody (Imgenex) as the first antibody and 1:5,000 diluted anti-mouse immunoglobulins conjugated with horseradish peroxidase (Wako Pure Chemicals) as the second antibody. The anti-Dnmt3a monoclonal antibody recognizes two Dnmt3a subtypes, Dnmt3a and Dnmt3a2 [36]. The chemiluminescence signals, which were obtained with SuperSignal West Pico Chemiluminescent Substrate (Pierce Chemical), were visualized by Chemi-Smart 3000 (Vilber Lourmat, Marne-la-Vallée, France, http://www.vilber.com). For reprobing, the blotted membrane was rinsed with Restore Western Blot Stripping Buffer (Pierce Chemical).

Preparation of Genomic DNA

Genomic DNA was extracted as previously described [37]. Briefly, cells were suspended in lysis buffer (150 mM EDTA, 10 mM Tris-HCl [pH 8.0], and 1% SDS) containing 10 mg/ml proteinase K (Merck, Darmstadt, Germany, http://www.merck.com). The mixture was incubated at 55°C for 20 minutes. After two phenol/chloroform/isoamyl alcohol (50:49:1) extractions, genomic DNA was precipitated in ethanol and dissolved in TE buffer (10 mM Tris-HCl, 1 mM EDTA [pH 8.0]).

Restriction Landmark Genomic Scanning

The restriction landmark genomic scanning (RLGS) was performed using the restriction enzyme combination of Not I, Pvu II, and Pst I as described previously [38]. Genomic DNA was treated with Klenow fragment (Takara, Kyoto, Japan, http://www.takara-bio.com) in the presence of dGTPαS, dCTPαS (GE Healthcare, Little Chalfont, Buckinghamshire, UK, http://www.gehealthcare.com), ddATP, and ddTTP (Takara) to prevent nonspecific labeling. After digestion by Not I as a landmark enzyme (Nippon Gene, Toyama, Japan, http://www.nippongene.com), cohesive ends were isotopically labeled with Sequenase Ver 2.0 (USB Corporation, Cleveland, http://www.usbweb.com) in the presence of [α-^{32}P]dCTP and [α-^{32}P]dGTP (GE Healthcare). Labeled DNA was digested by Pvu II (Nippon Gene) after first dimensional electrophoresis in 0.9% agarose disc gel. After in-gel digestion with Pst I (Nippon Gene), the DNA fragments were separated by a second dimensional electrophoresis in a polyacrylamide slab gel. The gel was then dried and exposed to x-ray film (Kodak, XAR 5; Eastman Kodak, Rochester, NY, http://www.kodak.com) for 2–3 weeks at −80°C.

Methylation-Sensitive Quantitative Real-Time PCR

DNA methylation status at *Sall3* locus was evaluated using methylation-sensitive quantitative real-time PCR as previously described [39]. Twenty nanograms of DNA treated with or without Not I was subjected to PCR with a primer pair amplifying a genomic fragment containing the Not I site. The methylation ratio was determined as the proportion of undigested DNA in Not I-treated DNA to that in Not I-untreated DNA. The amplification was monitored with SYBR green on an ABI Prism 7500 Sequence Detection System (Applied Biosystems) following the manufacturer's protocol. Initial DNA amount in the reaction mix was normalized with the value obtained with the primer pair of Xist1 that was designed to amplify fragments without the Not I site. More than three independent PCRs in triplicate were performed. The primers of Sall3 and Xist1 are as follows: Sall3: 5′-TTATACAACCTCGAACTAGCTGGG-3′ and 5′-GCATCCTGAATCCATGAACCCT-3′, Xist1: 5′-CACACACACCCTGCCCAATC-3′ and 5′-GGGATTCGCCTTGATTTGTGGT-3′.

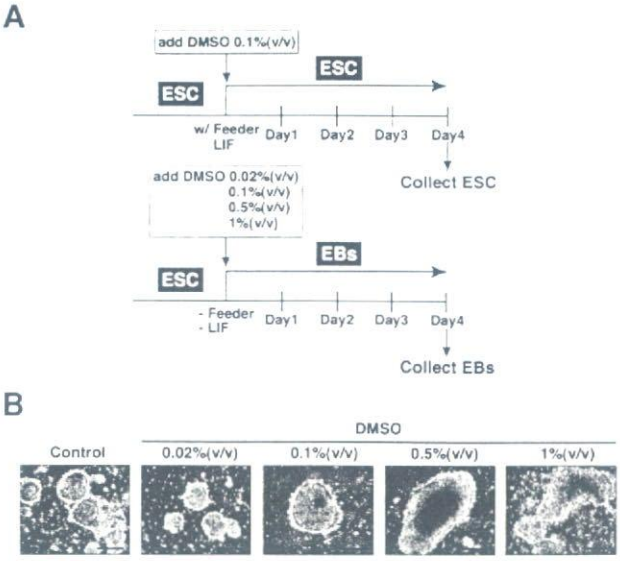

Figure 1. Culture of ESCs and of EBs with or without DMSO. **(A):** Cultivation scheme of mouse ESCs (MS12 line) and EBs. ESCs were cultured for 4 days in the presence of LIF and feeder layer with or without DMSO, or were induced to form EBs by removal of LIF and feeder layer, and were cultured for another 4 days with various concentrations of DMSO. **(B):** Micrographs of EBs cultured in medium containing DMSO. Concentrations are indicated above the images. Scale bars = 200 μm. Abbreviations: DMSO, dimethyl sulfoxide; EB, embryoid body; ESC, embryonic stem cell; LIF, leukemia inhibitory factor.

Southern Blot Hybridization

Genomic DNA that was digested with Msp I (Takara) or Hap II (Takara) was electrophoresed on a 0.8% agarose gel. After being hydrolyzed with 0.25 N HCl and denatured with 1.5 M NaCl in 0.5 N NaOH, DNA was transferred to a nylon membrane. The membrane was hybridized with pMO for endogenous C-type retrovirus (MoMuLV) (GenBank accession: NC_001501) or pMR150 for minor satellite repeats (X14469 and X07949), which was labeled with Gene Images random prime labeling module (GE Healthcare). The bound probes were detected by using Gene Images CDP-star detection module (GE Healthcare) with x-ray film (RX-U; Fuji, Kanagawa, Japan, http://www.fujifilm.com).

Results

DMSO Increases Expression of Dnmt3as in ESCs and EBs

ESCs, which were maintained without DMSO treatment, were cultured under differentiation conditions to form 4-day EBs in the absence or presence of various concentrations (0.02%–1%) of DMSO (Fig. 1A). In contrast to uniform spheres of EBs

cultured without DMSO, EBs with irregular shapes and increased sizes appeared in high concentrations (0.5%, 1%) of DMSO (Fig. 1B). In these phenotype changes of EBs induced by DMSO, we presume that epigenetic systems should be involved.

By semiquantitative RT-PCR, we examined expression of genes related to epigenetic systems such as Dnmts and histone modification enzymes. mRNA levels of Dnmt1 and Dnmt3b, which were expressed in ESCs and EBs, were not affected by DMSO treatment as judged by the densitometry of RT-PCR products (Fig. 2A). The fold changes of intensities of bands between the control and 1% DMSO-treated EBs showed 1.10 and 0.93 for Dnmt1 and Dnmt3b, respectively. In spite of the report that mDot1 mRNA was increased by DMSO treatment in mIMCD cells [25], mRNAs for histone methyltransferases (G9a, Suv39h1, Suv39h2, and mDot1), and a histone deacetylase, Sir2α, were expressed equally in ESCs as well as EBs at different DMSO concentrations. On the contrary, intensities of Dnmt3a in EBs, treated with 0.5% and 1% DMSO, increased almost double.

Real-time quantitative RT-PCR confirmed the increase of Dnmt3a mRNA (Fig. 2B). In ESCs, 0.1% of DMSO treatment caused a slight increase in the level of Dnmt3a mRNA. An approximately twofold increase in Dnmt3a mRNA was observed by differentiation of ESCs to EBs. In EBs, statistically significant increases in levels of Dnmt3a mRNA corresponded to increases in DMSO dosage.

To address the question whether Dnmt3a protein would increase coordinately with transcripts of Dnmt3a by DMSO treatment, Dnmt3a proteins in EBs were analyzed by Western blotting. Two distinct bands, which were detected by anti-Dnmt3a monoclonal antibody, indicated the expression of Dnmt3a and Dnmt3a2 in 4-day EBs. Both types of Dnmt3a protein levels in EBs treated with 0.5% and 1% DMSO increased to two times those in nontreated EBs (Fig. 2C). From this finding, taken together with upregulated mRNA level by DMSO treatment, it was clear that DMSO increased expression of Dnmt3as (Dnmt3a and Dnmt3a2).

DMSO Affects DNA Methylation Status of Repetitive Sequences in EBs

The mammalian genome consists of genic and nongenic regions, such as repetitive sequences, and the latter occupy a large part of the genome. Both regions are methylated de novo by Dnmt3as [40]. Minor satellite repeats, which are located in the centromeric regions, and endogenous retroviruses, which are interspersed in the mouse genome, are families of repetitive sequences. To assess the effects of DMSO (0.1%) on methylation levels in EBs, Southern blot was performed using probes for minor satellite repeats (pMR150) and endogenous C-type retroviruses (pMO) (Fig. 3). The differences in amounts of small fragments between lanes I, DNA digested by a DNA methylation-insensitive restriction enzyme, Msp I, and lanes II, digested by a methylation-sensitive enzyme, Hap II, indicate that these repetitive sequences were hypermethylated in EBs. The 0.1% DMSO treatment caused the disappearance of the small fragments of minor satellite and C-type retrovirus repeats in the EB genome (lanes III). These data indicated that DMSO prompted DNA methylation of these nongenic regions in the EBs.

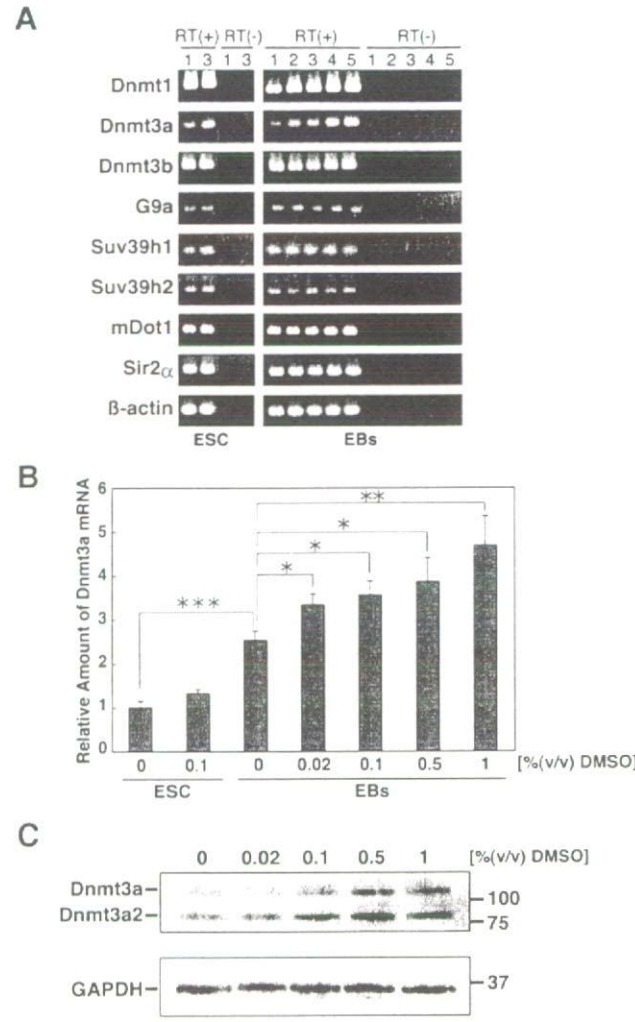

Figure 2. The effects of DMSO on expression of epigenetic factors in ESCs and EBs. **(A):** Expression of epigenetic factors in ESCs and EBs was analyzed by reverse transcription-polymerase chain reaction (RT-PCR). Reactions were carried out with [RT(+)] or without [RT(-)] reverse transcriptase. Primer sets are indicated to the left of the gel images. Concentrations (vol/vol) of DMSO were 0% (lane 1), 0.02% (lane 2), 0.1% (lane 3), 0.5% (lane 4), and 1% (lane 5). **(B):** Dnmt3a expression was analyzed by real-time quantitative RT-PCR. The value obtained in ESCs without DMSO was set to 1. Shaded blocks represent mean values, and standard error is represented by vertical bars. Differences between samples were analyzed by *t* test (*$p < .1$, **$p < .05$, ***$p < .005$ [$n = 3$]). **(C):** Dnmt3a protein expression was analyzed by Western blotting. The positions of proteins (left side) and molecular weights of the markers (right side) are shown. Abbreviations: DMSO, dimethyl sulfoxide; Dnmt, DNA methyltransferase; EB, embryoid body; ESC, embryonic stem cell; GAPDH, glyceraldehyde-3-phosphate dehydrogenase.

DMSO Affects Genome-Wide DNA Methylation Profiles of Genic Areas in EBs

Next, we focused on the effect of DMSO on DNA methylation at the genic region using the RLGS method. In the RLGS profile, the spot is visible when the corresponding cutting site of Not I, a methylation-sensitive restriction enzyme, is hypomethylated, whereas it is invisible when the site is hypermethylated. Most Not I sites are in CpG islands [41], which are characterized by high CG content and frequent CpG appearance [42], and are

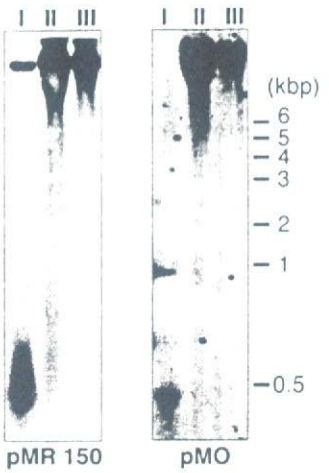

Figure 3. Effect of dimethyl sulfoxide (DMSO) on DNA methylation status of repetitive sequences. Msp I-digested genomic DNA from untreated EBs (lane I) and Hap II-digested genomic DNA from untreated (lane II) and 0.1% (vol/vol) DMSO-treated EBs (lane III) were subjected to Southern blot hybridization using probes for minor satellite repeats (pMR150) and endogenous C-type retrovirus repeats (pMO). Molecular weights are indicated on the right panel.

often localized at promoter regions of housekeeping genes and many tissue-specific genes [42–44]. Therefore, RLGS enables us to simultaneously analyze thousands of loci in genic regions.

The RLGS profiles, consisting of approximately 1,500 spots, were compared between control and 0.1% DMSO-treated EBs (Fig. 4A). In RLGS profiles of DMSO-treated EBs, 11 unique spots (T-DMR [DMSO] 1–11) emerged, indicating that DMSO induced hypomethylation of these 11 sites in EBs (Fig. 4B). In contrast, four spots (T-DMRs [DMSO] 12–15) disappeared in DMSO-treated EBs, indicating that DMSO caused hypermethylation of these four sites. Thus, 15 genomic loci were epigenetically affected by DMSO treatment, whereas thousands of loci remained unchanged (Fig. 4A, 4B).

We compared these 15 spots (T-DMRs [DMSO] 1–15) with T-DMRs that we previously identified [15, 16] (Fig. 5). The two spots, T-DMRs (DMSO) 2 and 12, were matched with T-DMRs 148 and 253, respectively, whereas the other 13 spots were novel. We defined them as T-DMRs 582 and 701–712, serially (Fig. 5). One of the matched spots is located in *Sall3* gene (T-DMR [DMSO] 2), which is specifically hypermethylated in the trophoblast lineage but hypomethylated in ESCs [31]. By methylation-sensitive PCR, DNA methylation status of this locus in DMSO-treated EBs was estimated to be approximately 3.5 times lower than that in EBs without DMSO (Fig. 4C).

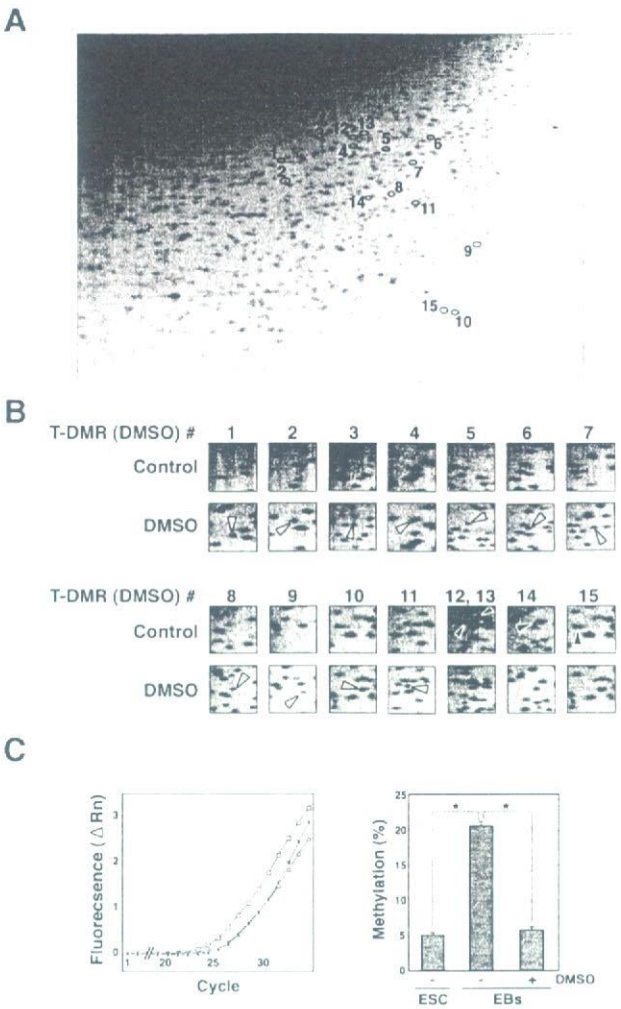

Figure 4. Analysis of genome-wide DNA methylation status in mouse EBs untreated or treated with DMSO and methylation status of *Sall3* locus. **(A):** RLGS profile obtained with genomic DNA of EBs treated with 0.1% (vol/vol) of DMSO. The 15 spots, which differentially appeared by treatment with DMSO, are marked with numbered circles. **(B):** Higher magnification of the RLGS profile. The 11 RLGS spots that emerged (i.e., hypomethylated) and the four spots that disappeared (i.e., hypermethylated) by DMSO treatment are indicated with white and black arrowheads, respectively. **(C):** Methylation-sensitive quantitative real-time PCR analysis for *Sall3* locus. Amplification curves with asterisks, circles, and squares represent Not I-treated genomic DNA of ESCs and of EBs with or without DMSO treatment, respectively (left panel). Methylation levels of *Sall3* locus were estimated as described in Materials and Methods. Differences between samples were statistically analyzed by *t* test (*$p < .001$, [ESCs: $n = 3$, EBs: $n = 4$]) (right panel). Abbreviations: DMSO, dimethyl sulfoxide; ΔRn, delta normalized reporter; EB, embryoid body; ESC, embryonic stem cell; PCR, polymerase chain reaction; RLGS, restriction landmark genomic scanning; T-DMR, tissue-dependent and differentially methylated region.

Discussion

The present study clearly demonstrates that DMSO has an impact on the epigenetic regulatory system, changes the genome-wide DNA methylation status, and induces formation of structurally abnormal EBs. Irreversible phenotypic changes in Friend cells were induced by DMSO [2, 3]. In animal cloning technology, DMSO improved the frequency of development to blastocyst stage and full term [5]. Because DNA methylation plays a critical role in mouse development and the definition of cell properties, change in genome-wide DNA methylation profiles induced by DMSO treatment may be responsible for these phenomena.

The human and mouse genomes contain 30,000–40,000 genes; however, genes occupy only a small percentage of the approximately 3×10^9 bp haploid genome. In contrast, 41%–48% of the mammalian genome is composed of nongenic repetitive elements, including satellites interspersed repeats such

T-DMR (DMSO) number	1	2	3	4	5	6	7	8	9	10	11	12	13	14	15
T-DMR number	582	148	701	702	703	704	705	706	707	708	709	253	710	711	712
ESC	○	○	○	○	○	○	○	○	○	○	○	●	●	●	○
EB 4day (control)	●	●	●	●	●	●	●	●	●	●	●	○	○	○	○
EB 4day (DMSO)	○	○	○	○	○	○	○	○	○	○	○	●	●	●	●

○: spot appeared on RLGS profile (unmethylated status)
●: no spot on RLGS profile (methylated status)

Figure 5. Matching of T-DMRs (DMSO) to previously identified T-DMRs. T-DMRs (DMSO) 1–15 (Fig. 4) were compared with previously identified T-DMRs by matching RLGS profiles. T-DMRs (DMSO) 2 and 12 correspond to T-DMRs 148 and 253 (which were previously identified), respectively. The 13 novel RLGS spots—T-DMRs (DMSO) 1, 3–11, and 13–15—were designated as T-DMRs 582 and 701–712, serially. Abbreviations: DMSO, dimethyl sulfoxide; EB, embryoid body; ESC, embryonic stem cell; RLGS, restriction landmark genomic scanning; T-DMR, tissue-dependent and differentially methylated region.

as retroviruses [45, 46]. A recent database analysis suggested that approximately half of all promoter regions are located in CpG islands [44]. We have identified many regions in CpG islands that have different methylation statuses depending on cell types and tissues, indicating that dynamic change in DNA methylation occurs during differentiation [15–17]. The present study demonstrated that DMSO impacts DNA methylation status genome-wide, including genic and nongenic regions of EBs differentiated from ESCs. Furthermore, hypermethylation as well as hypomethylation occurred at 15 independent genomic loci after DMSO treatment. However, note that there are approximately 15,500 CpG islands in the mouse genome [46], which suggests that the methylation status of many loci must be affected by DMSO.

Differentiation of ESCs to EBs causes both hypermethylation and hypomethylation at various loci genome-wide in mammals [16]. The effects of DMSO on DNA methylation status of CpG islands during differentiation are summarized in Figure 6. When ESCs differentiate to EBs, 34 loci were hypermethylated, and 30 loci were hypomethylated, whereas 203 spots were unchanged. Of 34 loci that typically became hypermethylated during differentiation of ESCs to EBs, 11 remained hypomethylated after DMSO treatment. Similarly, the DNA methylation status of three out of the 30 hypomethylated loci, and one out of the 203 unchanged loci was affected by DMSO treatment. Thus, DMSO induces alteration of DNA methylation status at selected loci and generates a unique DNA methylation profile of EBs, accompanying the abnormal phenotypes.

We demonstrated the upregulation of mRNA and protein expression in Dnmt3as by DMSO. Overexpression of Dnmt3as causes de novo hypermethylation of both genic and nongenic regions in vivo [40]. Abnormal expression of Dnmts has been observed in cancerous cells in which aberrant DNA methylation occurred; such expression includes an increase in DNMT1 and DNMT3b expression in various cancer cells [47] and a higher level of DNMT3a expression in leukemia [48, 49]. The preference of Dnmts for target loci within CpG islands was observed in ESCs [39]. Catalytic activities of Dnmt3a showed preference for nucleotide composition around the CpG sites [50]. Therefore, DMSO-induced increased expression of Dnmt3as should be involved in hypermethylation occurring at nongenic regions and selected gene loci of EB genome.

Despite increased expression of Dnmt3as and hypermethylation of the repetitive sequences and the selected loci, a number of hypomethylated loci (11 spots) are greater than that of hypermethylated loci (four spots) in genic regions (Fig. 4). In many cancer cells with epigenetic abnormalities, genomic DNA has shown to be globally hypomethylated with

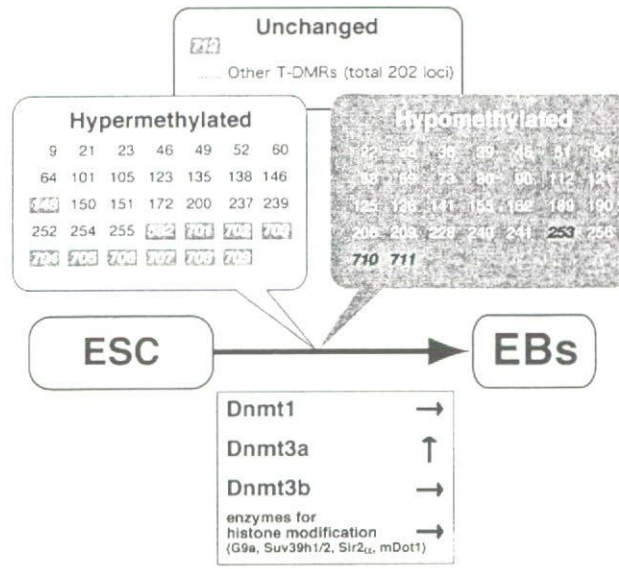

Figure 6. The impact of dimethyl sulfoxide (DMSO) on tissue-dependent and differentially methylated region (T-DMRs). This figure illustrates the T-DMRs that were hypermethylated, hypomethylated, or unchanged during the differentiation of ESCs into EBs. T-DMRs with methylation status affected by DMSO are in bold italics. Numbers with white letters in shaded square boxes and numbers with black letters in the shaded balloon represent hypomethylated and hypermethylated loci by DMSO, respectively. Abbreviations: Dnmt, DNA methyltransferase; EB, embryoid body; ESC, embryonic stem cell.

hypermethylation at selected genes. Such locus-specific DNA methylation status on genomic loci is contributed by complex combinations of Dnmts and other epigenetic regulators. Dnmt1 and Dnmt3s functionally cooperate with each other during methylation of genomic DNA [51, 52]. Methylation of DNA, however, was not solely regulated by Dnmts; chromatin configuration affects DNA methylation status and vice versa [20, 22–24]. Therefore, genome-wide alteration of the DNA methylation profile by DMSO should not be explained simply by the increased levels of Dnmt3as.

Conclusion

We conclude that DMSO upregulates expression of Dnmt3as and affects DNA methylation status at restricted loci accompanied with abnormal EB formation. Physiological and toxicological assessment of chemical agents at epigenetic levels is important, and analysis of genome-wide DNA methylation profiles will be useful in evaluating epimutagens.

ACKNOWLEDGMENTS

We thank Dr. Maddy Roberts and Chiaki Maeda for proofreading the original manuscript. This work was supported by the Program for Promotion of Basic Research Activities for Innovative Biosciences, Health Science Research Grant from the Ministry of Health, Labor and Welfare of Japan, and the Grant-in-aid for Scientific Research, Ministry of Education, Culture, Sports, Science and Technology, Japan (15208027, 15080202) (to K.S.).

DISCLOSURES

The authors indicate no potential conflicts of interest.

REFERENCES

1 Santos NC, Figueira-Coelho J, Martins-Silva J et al. Multidisciplinary utilization of dimethyl sulfoxide: Pharmacological, cellular, and molecular aspects. Biochem Pharmacol 2003;65:1035–1041.

2 Preisler HD, Giladi M. Differentiation of erythroleukemic cells in vitro: Irreversible induction by dimethyl sulfoxide (DMSO). J Cell Physiol 1975;85:537–546.

3 Gusella J, Geller R, Clarke B et al. Commitment to erythroid differentiation by friend erythroleukemia cells: A stochastic analysis. Cell 1976; 9:221–229.

4 Edwards MK, Harris JF, McBurney MW. Induced muscle differentiation in an embryonal carcinoma cell line. Mol Cell Biol 1983;3:2280–2286.

5 Wakayama T, Yanagimachi R. Effect of cytokinesis inhibitors, DMSO and the timing of oocyte activation on mouse cloning using cumulus cell nuclei. Reproduction 2001;122:49–60.

6 Hattori N, Nishino K, Ko YG et al. Epigenetic control of mouse Oct-4 gene expression in embryonic stem cells and trophoblast stem cells. J Biol Chem 2004;279:17063–17069.

7 Nishino K, Hattori N, Tanaka S et al. DNA methylation-mediated control of Sry gene expression in mouse gonadal development. J Biol Chem 2004;279:22306–22313.

8 Sinsheimer RL. The action of pancreatic deoxyribonuclease. II. Isomeric dinucleotides J Biol Chem 1955;215:579–583.

9 Russo VEA, Martienssen RA, Riggs AD. Introduction. In: Russo VEA, Martienssen RA, Riggs AD, eds. Epigenetic Mechanisms of Gene Regulation. Woodbury, NY: Cold Spring Harbor Laboratory Press, 1996: 1–4.

10 Bird AP, Wolffe AP. Methylation-induced repression–belts, braces, and chromatin. Cell 1999;99:451–454.

11 Bird A. DNA methylation patterns and epigenetic memory. Genes Dev 2002;16:6–21.

12 Lachner M, Jenuwein T. The many faces of histone lysine methylation. Curr Opin Cell Biol 2002;14:286–298.

13 Imamura T, Ohgane J, Ito S et al. CpG island of rat sphingosine kinase-1 gene: Tissue-dependent DNA methylation status and multiple alternative first exons. Genomics 2001;76:117–125.

14 Futscher BW, Oshiro MM, Wozniak RJ et al. Role for DNA methylation in the control of cell type specific maspin expression. Nat Genet 2002; 31:175–179.

15 Shiota K, Kogo Y, Ohgane J et al. Epigenetic marks by DNA methylation specific to stem, germ and somatic cells in mice. Genes Cells 2002;7:961–969.

16 Kremenskoy M, Kremenska Y, Ohgane J et al. Genome-wide analysis of DNA methylation status of CpG islands in embryoid bodies, teratomas, and fetuses. Biochem Biophys Res Commun 2003;311:884–890.

17 Shiota K. DNA methylation profiles of CpG islands for cellular differentiation and development in mammals. Cytogenet Genome Res 2004; 105:325–334.

18 Okano M, Xie S, Li E. Dnmt2 is not required for de novo and maintenance methylation of viral DNA in embryonic stem cells. Nucleic Acids Res 1998;26:2536–2540.

19 Hata K, Okano M, Lei H et al. Dnmt3L cooperates with the Dnmt3 family of de novo DNA methyltransferases to establish maternal imprints in mice. Development 2002;129:1983–1993.

20 Li E. Chromatin modification and epigenetic reprogramming in mammalian development. Nat Rev Genet 2002;3:662–673.

21 Chen T, Li E. Structure and function of eukaryotic DNA methyltransferases. Curr Top Dev Biol 2004;60:55–89.

22 Xin Z, Tachibana M, Guggiari M et al. Role of histone methyltransferase G9a in CpG methylation of the Prader-Willi syndrome imprinting center. J Biol Chem 2003;278:14996–15000.

23 Lehnertz B, Ueda Y, Derijck AA et al. Suv39h-mediated histone H3 lysine 9 methylation directs DNA methylation to major satellite repeats at pericentric heterochromatin. Curr Biol 2003;13:1192–1200.

24 Espada J, Ballestar E, Fraga MF et al. Human DNA methyltransferase 1 is required for maintenance of the histone H3 modification pattern. J Biol Chem 2004;279:37175–37184.

25 Zhang W, Hayashizaki Y, Kone BC. Structure and regulation of the mDot1 gene, a mouse histone H3 methyltransferase. Biochem J 2004; 377:641–651.

26 Vaquero A, Scher M, Lee D et al. Human SirT1 interacts with histone H1 and promotes formation of facultative heterochromatin. Mol Cell 2004; 16:93–105.

27 Hansen RS, Wijmenga C, Luo P et al. The DNMT3B DNA methyltransferase gene is mutated in the ICF immunodeficiency syndrome. Proc Natl Acad Sci U S A 1999;96:14412–14417.

28 Shahbazian MD, Zoghbi HY. Rett syndrome and MeCP2: Linking epigenetics and neuronal function. Am J Hum Genet 2002;71:1259–1272.

29 Ohgane J, Wakayama T, Kogo Y et al. DNA methylation variation in cloned mice. Genesis 2001;30:45–50.

30 Humpherys D, Eggan K, Akutsu H et al. Epigenetic instability in ES cells and cloned mice. Science 2001;293:95–97.

31 Ohgane J, Wakayama T, Senda S et al. The Sall3 locus is an epigenetic hotspot of aberrant DNA methylation associated with placentomegaly of cloned mice. Genes Cells 2004;9:253–260.

32 Jones PA, Baylin SB. The fundamental role of epigenetic events in cancer. Nat Rev Genet 2002;3:415–428.

33 Holliday R. Mutations and epimutations in mammalian cells. Mutat Res 1991;250:351–363.

34 O'Shea KS. Embryonic stem cell models of development. Anat Rec 1999;257:32–41.

35 Kawase E, Suemori H, Takahashi N et al. Strain difference in establishment of mouse embryonic stem (ES) cell lines. Int J Dev Biol 1994;38: 385–390.

36 Chen T, Ueda Y, Xie S et al. A novel Dnmt3a isoform produced from an alternative promoter localizes to euchromatin and its expression correlates with active de novo methylation. J Biol Chem 2002;277: 38746–38754.

37 Ohgane J, Aikawa J, Ogura A et al. Analysis of CpG islands of trophoblast giant cells by restriction landmark genomic scanning. Dev Genet 1998;22:132–140.

38 Ohgane J, Hattori N, Shiota K. Analysis of tissue-specific DNA methylation during development. Methods Mol Biol 2005;289:371–382.

39 Hattori N, Abe T, Hattori N et al. Preference of DNA methyltransferases for CpG islands in mouse embryonic stem cells. Genome Res 2004;14: 1733–1740.

40 Chen T, Ueda Y, Dodge JE et al. Establishment and maintenance of genomic methylation patterns in mouse embryonic stem cells by Dnmt3a and Dnmt3b. Mol Cell Biol 2003;23:5594–5605.

41 Fazzari MJ, Greally JM. Epigenomics: Beyond CpG islands. Nat Rev Genet 2004;5:446–455.

42 Gardiner-Garden M, Frommer M. CpG islands in vertebrate genomes. J Mol Biol 1987;196:261–282.

43 Larsen F, Gundersen G, Lopez R et al. CpG islands as gene markers in the human genome. Genomics 1992;13:1095–1107.

44 Suzuki Y, Tsunoda T, Sese J et al. Identification and characterization of the potential promoter regions of 1031 kinds of human genes. Genome Res 2001;11:677–684.

45 Lander ES, Linton LM, Birren B et al. Initial sequencing and analysis of the human genome. Nature 2001;409:860–921.

46 Waterston RH, Lindblad-Toh K, Birney E et al. Initial sequencing and comparative analysis of the mouse genome. Nature 2002;420:520–562.

47 Kanai Y, Ushijima S, Kondo Y et al. DNA methyltransferase expression and DNA methylation of CPG islands and peri-centromeric satellite regions in human colorectal and stomach cancers. Int J Cancer 2001;91: 205–212.

48 Mizuno S, Chijiwa T, Okamura T et al. Expression of DNA methyltransferases DNMT1, 3A, and 3B in normal hematopoiesis and in acute and chronic myelogenous leukemia. Blood 2001;97:1172–1179.

49 Tessema M, Langer F, Dingemann J et al. Aberrant methylation and impaired expression of the p15(INK4b) cell cycle regulatory gene in chronic myelomonocytic leukemia (CMML). Leukemia 2003;17:910–918.

50 Lin IG, Han L, Taghva A et al. Murine de novo methyltransferase Dnmt3a demonstrates strand asymmetry and site preference in the methylation of DNA in vitro. Mol Cell Biol 2002;22:704–723.

51 Liang G, Chan MF, Tomigahara Y et al. Cooperativity between DNA methyltransferases in the maintenance methylation of repetitive elements. Mol Cell Biol 2002;22:480–491.

52 Kim GD, Ni J, Kelesoglu N et al. Co-operation and communication between the human maintenance and de novo DNA (cytosine-5) methyltransferases. Embo J 2002;21:4183–4195.

Development of an Analytical Method for Perfluorochemicals in Human Plasma and Blood by Liquid Chromatography-Tandem Mass Spectrometry Coupled with Solid-Phase Extraction Using a Column-Switching Technique

Hisao Nakata[1], Ayako Nakata[1], Migaku Kawaguchi[1], Yusuke Iwasaki[1], Rie Ito[1], Koichi Saito[1], Hiroyuki Nakazawa[1]

[1]Hoshi University

Introduction

Perfluorochemicals (PFCs) are man-made chemicals used as surfactants, polymers, plastic additives, and so on. Their amphiphilic character and their thermal, biological, and chemical stability make them useful for many purposes [1]. On the other hand, evidence of toxic effects and environmental pollution was reported and discussed [2]. Previous reports for the measurement of PFCs in human blood samples were performed by liquid chromatography-mass spectrometry (LC/MS) and LC/MS/MS with liquid-liquid extraction or solid-phase extraction [3-5]. However, these methods sometimes required a complicated process for extraction, clean-up and concentration of these compounds. Therefore, we have developed a simple and rapid method for the determination of PFCs such as perfluorooctanesulfonic acid (PFOS), perfluorooctanesulfonamide (PFOSA), perfluorooctanoic acid (PFOA), perfluorononanoic acid (PFNA) and perfluorodecanoic acid (PFDA) in human plasma and whole blood by liquid chromatography-tandem mass spectrometry (LC/MS/MS) coupled with solid-phase extraction using column-switching. The PFCs in human plasma and whole blood samples can be measured by LC/MS/MS with an online solid-phase extraction, only after deproteination with acetonitrile. The method enables the precise determination of standards and can be applied to the determination of PFOS, PFOSA, PFOA, PFNA and PFDA in human plasma and whole blood for monitoring human exposure.

Materials and methods

PFOS (M.W. 538.23, 98%), PFOA (M.W. 414.07, >90%) and PFNA (M.W. 464.08, 95%) were obtained from FlukaChemie AG, Buchs, Switzerland. PFOSA (M.W. 499.14, 97%) and PFDA (M.W. 514.08, 97%) were purchased from ABCR GmbH & Co. KG, ImSchlehert and Lancaster Co. Inc., Morecambe, England, respectively. Perfluoroheptanoic acid (PFHpA, 99%) and 1H,1H, 2H, 2H-perfluorooctaneslufonic acid (THPFOS, >90%) that had been used as an internal standard were purchased Sigma Aldrich Laboratories, Inc., St. Louis, MO. and SynQuest lab. Inc., America, respectively.

Instrumentation and analytical conditions of column switching LC/MS/MS coupled with solid-phase extraction.Liquid chromatography-tandem mass spectrometry was performed using a Waters Quattro Micro system. Separation was achieved on an Inertsil ODS-3 column (2.1 x 50 mm, 5 um, GL Sciences Inc., Tokyo, Japan) with a Mightysil RP-18 GP pre-column (2.0 x 5 mm, 5 um, Kanto Chemical Inc., Osaka, Japan). The column oven was maintained at 40°C. The column-switching LC/MS/MS coupled with an on-line extraction system consisted of this LC/MS/MS combined with an LC pump (Shimadzu LC-10ADvp pump: Shimadzu, Kyoto, Japan) and Waters Oasis HLB extraction column (20 x 2.1 mm, 25 um). After a 50 ul sample was injected by an auto-sampler, it was loaded onto the extraction column by flowing 50 mM acetate buffer (pH=4.7)/methanol (90/10, v/v) at a flow rate of 1.0 ml/min. The valve was switched 5 min after sample injection. The sample was eluted by back-flashing extraction column to the analytical column and was introduced to MS/MS. The separation was carried out using a mobile phase of 1.0 mM ammonium acetate in water/acetonitrile (v/v) at a flow rate of 0.2 ml/min. The gradient mode was as follows: 5-12 min using a linear increase from 45 to 85% acetonitrile solution, and holding at 85%. The conditions of MS/MS were as follows: the desolvation and source temperatures were set at 350°C and 100°C, respectively; the capillary was held at a potential of 600 V relative to the counter electrode in the negative-ion mode for all compounds. The cone and desolvation gas flow were 50 and 350 l/hr. The cone and collision voltage were 60 and 65 V for PFOS, and 45 and 35 V for PFOSA, 30 and 18 V for PFOA, 30 and 20 V for PFNA, 30 and 22 V for PFDA, 28 and 18 V for PFHpA, and 35 and 37 V for THPFOS.

Sample preparation.The 0.1 ml of human plasma and whole blood samples were added to 0.3 ml of internal standard solution with acetonitrile. The mixed plasma sample was centrifuged at 1450 x g for 10 min and whole blood

sample was centrifuged 10000 x g for 10 min after sonication for 10 min. The supernatant was removed to the polypropylene tube. The filtered sample solution was determined by the column switching LC/MS/MS.

Results and discussions

Column-switching LC/MS/MS coupled with an on-line extraction system. In the mass spectral analysis using MS/MS system, both molecular and fragment ions were observed as the major peaks. The precursor ions were set *m/z* 499 for PFOS, *m/z* 498 for PFOSA, *m/z* 369 for PFOA, *m/z* 419 for PFNA, *m/z* 469 for PFDA, *m/z* 319 for PFHpA and *m/z* 427 for THPFOS, respectively. The product ions were set *m/z* 499→80 for PFOS, *m/z* 498→78 for PFOSA, *m/z* 369→169 for PFOA, *m/z* 419→169 for PFNA, *m/z* 469→169 for PFDA, *m/z* 319→169 for PFHpA and *m/z* 427→81 for THPFOS, respectively. The capillary voltage and mobile phase were optimized by using set monitoring ion. As for the capillary voltage, the peak area became the maximum in 600 V (Figure 1). The effect of the mobile phase ammonium acetate concentration was shown in Figure 2. When the 1.0 mM ammonium acetate was added to mobile phase, the peak area was the maximum.

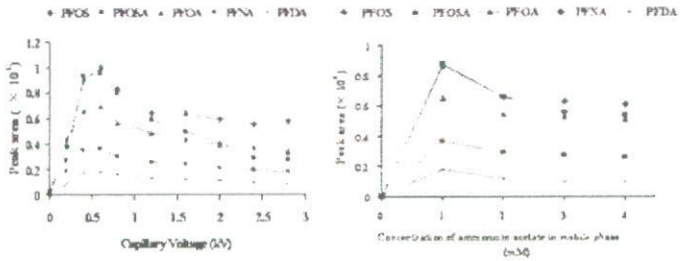

Internal standard. Recently, it was recommended that ^{13}C-labeled isotope be used as internal standard for MS. However, obtaining the ^{13}C-labeled isotope of PFCs was very difficult. We evaluated PFHpA and THPFOS as internal standards. PFHpA and THPFOS were evaluated by comparing the PFCs recoveries in human plasma samples spiked with analytes at 10 ng/ml (Figure 3). The recoveries of analytes using THPFOS as internal standard were 43.7 to 53.3%. However, the recoveries of analytes using PFHpA as internal standard were 91.0 to 110%. Therefore, we used PFHpA as internal standard.

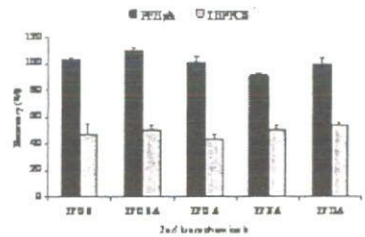

Validation and recovery test. The calculated detection limits of PFOS, PFOSA, PFOA, PFNA and PFDA with a signal-to-noise ratio of 3:1 were 0.02, 0.02, 0.025, 0.03 and 0.03 ng/ml, respectively. In addition, the calculated method quantification limits of PFOS, PFOSA, PFOA, PFNA and PFDA were 0.5 ng/ml. The calibration curves (0.5-100 ng/ml) were rectilinear with over 0.999. The average recoveries of PFOS, PFOSA, PFOA, PFNA and PFDA in human plasma were in the range of 93.3 to 105% (RSD: 3.0-8.9%, n=6) (Table 1). Obtaining human whole blood was very difficult. Therefore, horse whole blood was examined instead of human whole blood. The average of recoveries in horse whole blood were in the range of 92.8 to 108% (RSD: 2.5-7.9%, n=6) (Table 2).The method enables the precise determination of standards and can be applied to the determination of PFOS, PFOSA, PFOA, PFNA and PFDA in human plasma and whole blood for monitoring human exposure.

Table 1 Recovery levels of PFOS, PFOSA, PFOA, PFNA and PFDA in human plasma sample spiked with the PFCs and internal standard

Compound	Spiked amount (ng/mL, human plasma sample)	Average recovery(%)	RSD (%)
PFOS	5	99.3	3.0
	50	97.5	6.3
PFOSA	1	98.3	4.2
	10	103	4.2
PFOA	1	103	8.9
	10	97.3	4.8
PFNA	1	98.7	8.4
	10	94.7	3.1
PFDA	1	98.3	8.7
	10	103	4.7

(n=6)

Table 2 Recovery levels of PFOS, PFOSA, PFOA, PFNA and PFDA in horse whole blood sample spiked with the PFCs and internal standard

Compound	Spiked amount (ng/mL, horse whole blood sample)	Average recovery(%)	RSD (%)
PFOS	5	97.0	2.5
	50	102	4.5
PFOSA	1	92.9	3.3
	10	102	7.1
PFOA	1	103	5.1
	10	96.3	3.7
PFNA	1	102	7.9
	10	100	2.1
PFDA	1	99.5	7.5
	10	102	4.7

(n=6)

Reference

1. A. Karrman, B. B. Van, U. Jarnberg, L. Hardell, G. Lindstrom, *Anal. Chem.*, **77**, 864 (2005)

2. M. E. Austin, B. S. Kasturi, M. Barber, K. Kannan, P. MohanKumar, S. M. J. MohanKumar, *Environ. Health. Perspect.*, **111** (2003)

3. G. W. Olsen, K. J. Hansen, L. A. Stevenson, J. M. Burris, J. H. Mandel, *Environ. Sci. Technol.* **37**, 888(2003)

4. K. Kannan, S. Corcolini, J. Falandysz, G. Fillmann, K. S. Kumar, B. G. Loganathan, M. A. Mohd, J. Olivero, J. H. Yang, K. M. Aldous, *Environ. Sci. Technol.*, **38**, 4489 (2004)

5. Z. Kuklenyik, J. A. Reich, J. S. Tully, A. M. Calafat, *Environ. Sci. Technol.* **38**, 4489 (2004)

BUNSEKI KAGAKU Vol. 54, No. 9, pp. 877–884 (2005)

報　文

オンライン固相抽出-高速液体クロマトグラフィー/タンデム質量分析計を用いるヒト血しょう中有機フッ素系化合物の一斉分析法の開発

仲田　尚生[1]，中田　彩子[1]，岡田　文雄[1]，伊藤　里恵[1]，
井之上浩一[1]，斉藤　貢一[1]，中澤　裕之*[1]

Development of Online Solid-Phase Extraction-HPLC/MS/MS Method for the Determination of Perfluorochemicals in Human Plasma

Hisao NAKATA[1], Ayako NAKATA[1], Fumio OKADA[1], Rie ITO[1],
Koichi INOUE[1], Koichi SAITO[1] and Hiroyuki NAKAZAWA[1]

[1] Department of Analytical Chemistry, Hoshi University, 2-4-41, Ebara, Shinagawa-ku, Tokyo 142-8501

(Received 15 April 2005, Accepted 26 July 2005)

A method for determining perfluorochemicals (PFCs) such as perfluorooctanesulfonic acid (PFOS), paerfluorooctane slufoneamide (PFOSA), perfluorooctanoic acid (PFOA), perfluorononanoic acid (PFNA) and perfluorodecanoic acid (PFDA), in human plasma samples was developed by online solid-phase extraction-HPLC/MS/MS, only after deproteination with acetonitrile. The limits of detection of PFOS, PFOSA, PFOA, PFNA and PFDA in human plasma at a signal to noise (ratio of 3) were 0.08～0.14 ng/ml, and the limits of quantitation of PFOS, PFOSA, PFOA, PFNA and PFDA in human plasma were 0.50 ng/ml. The average recoveries of PFOS, PFOSA, PFOA, PFNA and PFDA ranged from 93.3 to 105% (RSD, 3.0～8.9%; $n = 6$). This method is more rapid and accurate, compared with the column-switching HPLC/MS method presented in previous reports[18][19]. The developed method can be applied to the determination of PFOS, PFOSA, PFOA, PFNA and PFDA in human plasma samples for monitoring human exposure.

Keywords : perfluorooctanesulfonic acid; perfluorochemicals; MS/MS; human plasma; column-switching.

1　緒　　言

近年，新たな環境汚染物質として，パーフルオロオクタンスルホン酸（PFOS）を代表としたパーフルオロ化合物（PFCs）が注目されている．PFOSは，水にも油にも溶けやすい性質から界面活性剤として利用され，近年までに撥水剤，消火剤，潤滑油及び消泡剤等として用いられている．また，パーフルオロオクタン酸（PFOA）においては，テフロン加工製品にも応用されていることから，PFCsは，我々の生活環境中で広範囲に存在している．Fig. 1にこれらPFCsの構造を示す．直鎖状に並んだ炭素原子すべてにフッ素原子が結合しており，末端にスルホン酸基又はカルボン酸基を有する構造をしている．炭素原子とフッ素原子の結合は非常に強いため，PFOSは，極めて安定な化学物質であると考えられている．この安定性によりPFCsは，河川水，海洋性哺乳類，魚類及び鳥類等，生態系で分解することなく，長期にわたり残留することが報告されている[1)～5)]．また，毒性としては，実験動物に対する催奇形性，甲状腺ホルモンへの影響[6)7)]，ペルオキシソーム増殖作用[8)～10)]が報告されていることから次世代への影響や発がん作用，コレステロール代謝撹乱作用等が懸念されている．また，PFOAは実験動物において血しょうタンパク質と結

[1] 星薬科大学薬品分析化学教室：142-8501　東京都品川区荏原2-4-41

CF_3-$(CF_2)_7$-SO_3^- **PFOS**

CF_3-$(CF_2)_7$-COOH **PFOA**

CF_3-$(CF_2)_7$-SO_2NH_2 **PFOSA**

CF_3-$(CF_2)_8$-COOH **PFNA**

CF_3-$(CF_2)_5$-$CH_2CH_2SO_3^-$ **THPFOS(I.S.)**

CF_3-$(CF_2)_9$-COOH **PFDA**

CF_3-$(CF_2)_6$-COOH **PFHpA(I.S.)**

Fig. 1 Structures of PFCs and internal standards
PFOS: perfluorooctanesulfonic acid; PFOSA: perfluorooctanesulfonamide; PFOA: perfluorooctanoic acid; PFNA: perfluorononanoic acid; PFDA: perfluorodecanoic acid; PFHpA: perfluoroheptanoic acid; THPOS: 1*H*,1*H*,2*H*,2*H*-perfluorooctaneslufonic acid

合して血液中に蓄積しているという報告がある[11][12]．それ故 PFCs による生態系及びヒトへのリスク評価を行うためにサーベイランスが必要となっている．近年，国内において PFCs は，環境モニタリングが実施されている[13]が，ヒトへの暴露調査は，いまだほとんど行われていない．

現在，報告されている生体試料中 PFCs の測定は，主に高速液体クロマトグラフィー/質量分析計（HPLC/MS）及び高速液体クロマトグラフィー/タンデム質量分析計（HPLC/MS/MS）が用いられている[14]~[19]．しかしヒトへの暴露実態を正確に把握するためには，より精度の高い HPLC/MS/MS を用いる方が望ましいとされている．また，試料前処理法には，液-液抽出法[5][14][15]，固相抽出法[16][17]，カラムスイッチング法[18][19]が報告されている．液-液抽出法及び固相抽出法は，煩雑な操作を必要とし，多検体処理能に乏しい．また，先に報告したカラムスイッチング-HPLC/MS 法[18][19]では，簡便な操作ではあるが，分析時間が 30 分と長く，回収率及び分析精度がやや乏しい．そこで本研究では，簡便かつ多検体処理能を有する前処理法であるオンライン固相抽出法を採用し，高精度・高選択性な機能を有する HPLC/MS/MS を用いることにより，迅速かつ高感度・高精度な血しょう試料中 PFCs の一斉分析法を開発した．

2 実　　験

2・1 試　薬

パーフルオロオクタンスルホン酸（PFOS，>98%），パーフルオロオクタン酸（PFOA，>90%），パーフルオロノナン酸（PFNA，>98%）は Fulka 製を用いた．パーフルオロオクタンスルホンアミド（PFOSA，97%）は ABCR GmbH & Co.KG 製，パーフルオロデカン酸（PFDA，97%）は Lancaster 製を用いた．内標準物質として用いたパーフルオロヘプタン酸（PFHpA，99%）は Aldrich 製，1*H*,1*H*,2*H*,2*H*-パーフルオロオクタンスルホン酸（THPFOS，>90%）は SynQuest 製を用いた．精度管理用凍結乾燥プール血清コンセーラは，日水製薬製を用いた．超純水は日本ミリポア製 Milli-Q の超純水装置で調製したものを用いた．アセトニトリル，メタノールは，和光純薬製 HPLC 用及び残留農薬試験用を使用した．ナイロンメンブランフィルター（0.2 μm，13 mm）は，日本ポール製を用いた．

2・2 標準溶液の調製

各標準品をアセトニトリルに溶解させ，1.0 mg/ml の溶液を調製し，0.50～100 ng/ml の範囲で標準溶液を水/アセトニトリル = 50/50（v/v）で適宜希釈して測定用試料を調製した．

2・3 装置及び分析条件

HPLC/MS/MS は，Waters 製 Quattro micro システムを用いた．インジェクションボリュームを 50 μl とし，ガードカラムに関東化学製の Mightysil RP-18 GP プレカラム（2.0 mm × 5 mm，5 μm）を用い，分析カラムに GL サイエンス製 Inertsil ODS-3（2.1 mm × 50 mm，5 μm）を使用した．また，カラムオーブンは 40℃ に設定した．

オンライン固相抽出法の条件は，送液ポンプに島津製 LC-10ADvp pump を用い，固相カートリッジとしては，Waters 製 Oasis HLB extraction column（20 mm × 2.1 mm，25 μm）を使用した．構築したオンライン固相抽出システムを Fig. 2 に，操作プログラムを Table 1 に示す．オートサンプラーにより試料溶液を注入後，5 分間 50 mM 酢酸・酢酸アンモニウム緩衝液（pH = 4.7）/メタノール（90/10，v/v）を Pump 1 より送液することで，固相抽出カートリッジ上で測定対象物質の濃縮とクリーンアップを行った．次に六方バルブを切り替え，Pump 2 から 1 mM 酢酸アンモニウムを添加した水/アセトニトリル混液をバックフラッシュ法によりグラジエント溶出することで，測定対象物質を固相抽出カートリッジから溶出させ，分離部及び検出部に導入した．

MS/MS のイオン化法は，エレクトロスプレーイオン化法（ESI）のネガティブイオンモードを採用し，検量線及び実試料の測定は，Multipul Reaction Monitoring（MRM）モードで行った．MS/MS 条件としては，デソルベーション温度及びソース温度をそれぞれ 350℃，100℃ とし，コーンガス流量及びデソルベーションガス流量を 50 l/hr，

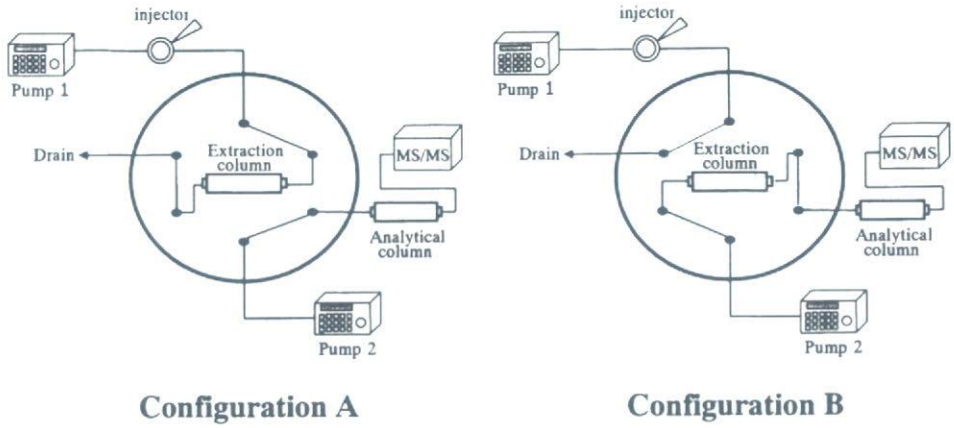

Fig. 2　Schematic diagram of the column-switching HPLC/MS/MS system
Configuration A: sample loading and washing; Configuration B: sample eluting

Table 1　Time program of column-switching HPLC/MS/MS coupled with on-line extraction condition

Time/min	Column position[a]	Mobile phase	
		Pump 1[b] (A-B, v/v)	Pump 2[c] (A-B-C, v/v)
0.0	Configuration A	90 : 10	54 : 1 : 45
5.0	Configuration B	90 : 10	54 : 1 : 45
10.0	Configuration A		
12.0		90 : 10	14 : 1 : 85
14.9		90 : 10	14 : 1 : 85
15.0		90 : 10	54 : 1 : 45

a) Configuration A and B are shown in Fig. 2; b) Pump 1 solvent: (A) 50 mM Ammonium acetate buffer (pH-4.7), (B) Methanol; c) Pump 2 solvent: (A) Water, (B) 100 mM Ammonium acetate, (C) Acetnitrile

350 l/hr とした．また，キャピラリー電圧を−600 V に設定した．コーン電圧及びコリジョンエネルギーを PFOS: −60 V，65 eV，PFOSA: −45 V，35 eV，PFOA: −30 V，18 eV，PFNA: −30 V，20 eV，PFDA: −30 V，22 eV，PFHpA: −28 V，18 eV，THPFOS: −35 V，37 eV に設定した時，モニタリングイオンはそれぞれ，PFOS: m/z 499 → 80，PFOSA: m/z 498 → 78，PFOA: m/z 369 → 169，PFNA: m/z 419 → 169，PFDA: m/z 469 → 169，PFHpA: m/z 319 → 169，THPFOS: m/z 427 → 81 となった．

測定対象物質の分離は，逆相分配モードの ODS (octadecyl silica) カラムを用い，1 mM 酢酸アンモニウムを添加した水/アセトニトリル (v/v) 混液を移動相として，流量 0.2 ml/min で送液し，測定時間 5〜12 分にかけて，アセトニトリル含量を 45〜85% にグラジエント溶出して行った．

2・4　ヒト血しょう試料

本研究遂行に当たり，血しょう試料の採取は提供対象者に対する人権擁護上の配慮，研究に対する利益・不利益等の説明を行い，インフォームドコンセントを得た．また，血しょう試料は，−80℃ で保存し，分析直前に室温で自然解凍した．ボランティアは，男女各 3 名ずつの健常人であった．

2・5　測定試料の調製法

0.1 ml のヒト血しょうに対して，内標準物質を含むアセトニトリル溶液を 0.2 ml 加えた．よくかくはん後，3000 rpm で 10 分間，遠心分離を行った．遠心分離後，上澄みをナイロンメンブランフィルター (0.2 μm) に通し，測定試料とした．

3　結果及び考察

3・1　オンライン固相抽出条件の検討

オンライン固相抽出法における溶離液の検討を行った．まず，水/メタノール (v/v) 混液について検討したところ，実試料と標準溶液の間において，保持時間にずれが生じた．この原因としては，固相抽出カートリッジ上での保持挙動が pH に依存するため，実試料中 PFCs の保持・溶出挙動が標準溶液と異なるためと考えられた．そこで，移動相に 50 mM 酢酸・酢酸アンモニウム緩衝液 (pH = 4.7)/メタノール (v/v) 混液を用いたところ，保持時間を一定に保つことが可能となった．また，Fig. 3 に 50 mM 酢酸・酢酸アンモニウム緩衝液 (pH = 4.7)/メタノール (v/v) の混合比率の検討を示す．メタノール含量が少ないほど，測定対象化合物のピーク面積は大きくなる傾向にあるが，メタノールを 10% 含む時点でほぼプラトーとなったので，最適混合比率を 50 mM 酢酸・酢酸アンモニウム

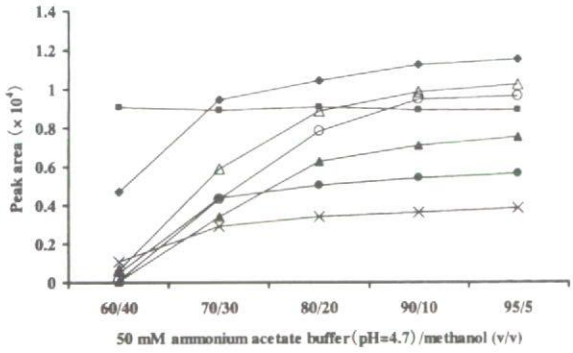

Fig. 3 Effect of the mobile phase composition on the peak area of PFCs
◆: PFOS; ■: PFOSA; ▲: PFOA; ●: PFNA; ×: PFDA; ○: PFHpA; △: THPFOS

緩衝液（pH = 4.7）/メタノール = 90/10（v/v）とした．

3・2 MS/MS 測定条件の検討

PFCs5 種類の標準品を用いて，MS/MS のイオン化について検討した．測定対象物質のマススペクトルを Fig. 4 に示す．イオン化法に ESI 法を採用し，ネガティブイオンモードで測定したところ，PFOS においては $[M-K]^-$ イオンの m/z 499，PFOSA，PFOA，PFNA，PFDA，PFHpA 及び THPFOS に関しては，$[M-H]^-$ イオンである m/z 498，413，463，513，363，427 の分子量関連イオンピークがそれぞれ確認された．この結果より，PFOS，PFOSA 及び THPFOS に関しては，m/z 499，498，427 をプレカーサーイオンとした．しかし，PFOA，PFNA，PFDA 及び PFHpA に関しては，$[M-H]^-$ イオンに比べ，$[M-COOH]^-$ イオンの強度が強かったため，プレカーサーイオンをそれぞれ，$[M-COOH]^-$ イオンである m/z 369，419，468，319 に設定した．またプレカーサーイオンが開裂することで生じるプロダクトイオンは，それぞれ PFOS: m/z 499 → 80，PFOSA: m/z 498 → 78，PFOA: m/z 369 → 169，PFNA: m/z 419 → 169，PFDA: m/z 469 → 169，PFHpA: m/z 319 → 169，THPFOS: m/z 427 → 81 とした．

設定したモニタリングイオンを用い，キャピラリー電圧のイオン強度に及ぼす影響について検討した．その結果を Fig. 5 に示す．キャピラリー電圧は −600 V の時，測定対象化合物すべてにおいて最大のピーク面積が得られた．また，一般的に MS や MS/MS を用いて測定をする際，揮発性の酸や塩基を少量加えることによりイオン化効率が上昇することが知られている．そこで今回，PFCs のイオン化効率を上昇させるため，酢酸アンモニウムの添加濃度を検討した（Fig. 6）．その結果，酢酸アンモニウムを 1 mM 添加した時に測定対象化合物のイオン強度が最大値を示した．

3・3 オンライン固相抽出-HPLC/MS/MS 測定条件の検討

得られた条件を用い，PFCs5 種類の標準品の測定を行った．Fig. 7（a）に示したクロマトグラムのようにすべての化合物を 15 分以内に良好に分離した．同様に血しょう試料に測定対象物質を 10 ng/ml となるように添加したクロマトグラムにおいても，他の夾雑物質の影響を受けることなく良好に相互分離することが可能であった［Fig. 7（b）］．また，血しょう試料における検出限界（$S/N = 3$）を求めたところ，それぞれ PFOS: 0.08 ng/ml，PFOSA: 0.11 ng/ml，PFOA: 0.11 ng/ml，PFNA: 0.10 ng/ml，PFDA: 0.14 ng/ml であった．定量限界は，すべての化合物を明瞭に測定することができる 0.50 ng/ml（$S/N > 10$）とした．

3・4 内標準物質の検討

近年，MS や MS/MS を用いた測定は，重水素置換体や ^{13}C 標識体等の安定同位体を用い，内標準法により測定が行われている．しかし，PFCs においては，重水素置換体や ^{13}C 標識体等の安定同位体の入手が困難なことから，内標準物質として PFOS 類似化合物が多く用いられている[15)17)]．そこで，今回は，従来多くの研究報告で用いられている PFHpA 及び THPFOS に着目した．標準溶液 0.1 ml に内標準物質含有アセトニトリル 0.2 ml を加え，よくかくはんした溶液を測定試料とし，検量線を作成したところ，0.50 ～ 100 ng/ml の範囲で良好な直線性（$r = 0.999$ 以上）を得ることができた．しかし，精度管理用プール血清コンセーラに測定対象物質が 10 ng/ml となるように添加して，回収率を求めた結果，PFHpA を内標準物質として用いた場合の回収率は，91.0% 以上と良好な結果を得ることができたが，THPFOS を用いた時，回収率 43.7 ～ 53.7% と良好な結果を得ることができなかった．THPFOS を用いた時に回収率が低減した原因としては，血清試料中の共存物質のマトリックス効果により，測定対象物質に比べ THPFOS のイオン強度が増加してしまったためと考えられる．これらの結果より，内標準物質として PFHpA を用いることにした．

3・5 添加回収試験

内標準物質に PFHpA を用い，ヒト血しょうにおける添加回収試験を行った．添加回収試験は，まず各測定対象化合物を異なる濃度レベルで添加した血しょう試料 0.1 ml に PFHpA 含有アセトニトリル 0.2 ml を加え，よくかくはんし，3000 rpm で 10 分間遠心分離を行った．次いで，上澄みをナイロンメンブランフィルター（0.2 μm）に通し，その沪液を測定して，回収率を算出した．その結果，平均回収率 93.3% 以上［相対標準偏差（RSD）≦ 8.9%］と良

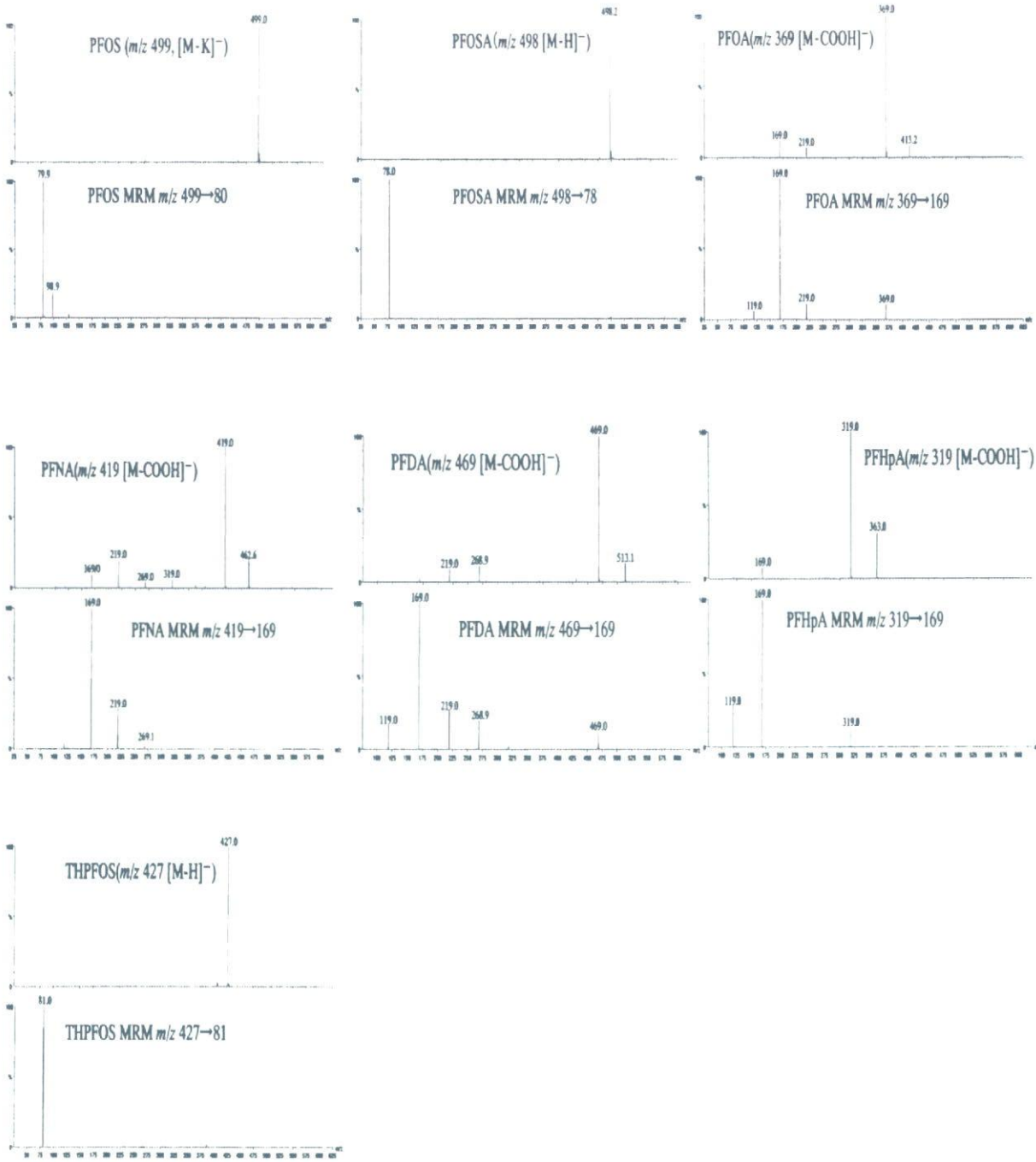

Fig. 4　Mass spectra of PFCs and internal standards
precursor ion spectrum : above ; product ion spectrum : below

好な結果を得ることができた（Table 2）.

本法を健常人6人に適用し，血しょう中の PFCs を測定した（Table 3）．その結果，すべての検体から PFOS 及び PFOA を検出することができた．PFOS 濃度は 2.1～21.3 ng/ml の範囲で，PFOA 濃度は 0.7～4.6 ng/ml の範囲で存在した．また，PFNA に関しても 3 検体から 0.6～1.0 ng/ml の範囲で検出することができた．これらの濃度は，既に報告されているヒト血しょう中の PFCs の濃度[15]と比較し，ほぼ同レベルであったことから，本法は，ヒト血液試料中 PFCs の定量に応用可能であることが認められた．

4　結　　言

本分析法では，前処理法にオンライン固相抽出法を用いることで，除タンパクのみという簡便な操作で PFCs の測

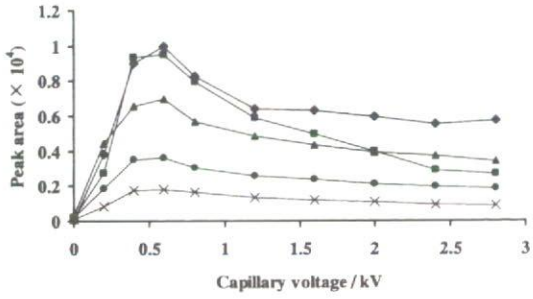

Fig. 5 Effect of capillary voltage on the peak area of PFCs

◆: PFOS; ■: PFOSA; ▲: PFOA; ●: PFNA; ×: PFDA

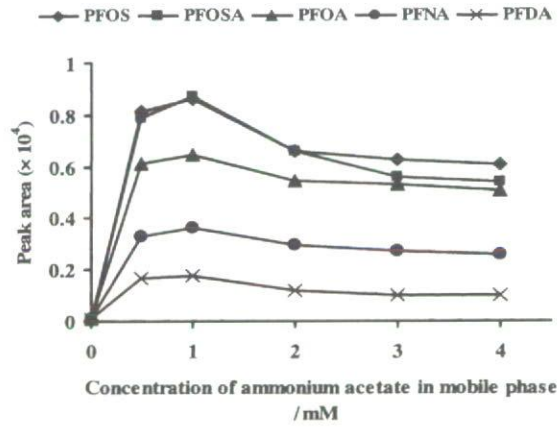

Fig. 6 Effect of concentration of ammonium acetate in mobile phase on the peak area of PFCs

◆: PFOS; ■: PFOSA; ▲: PFOA; ●: PFNA; ×: PFDA

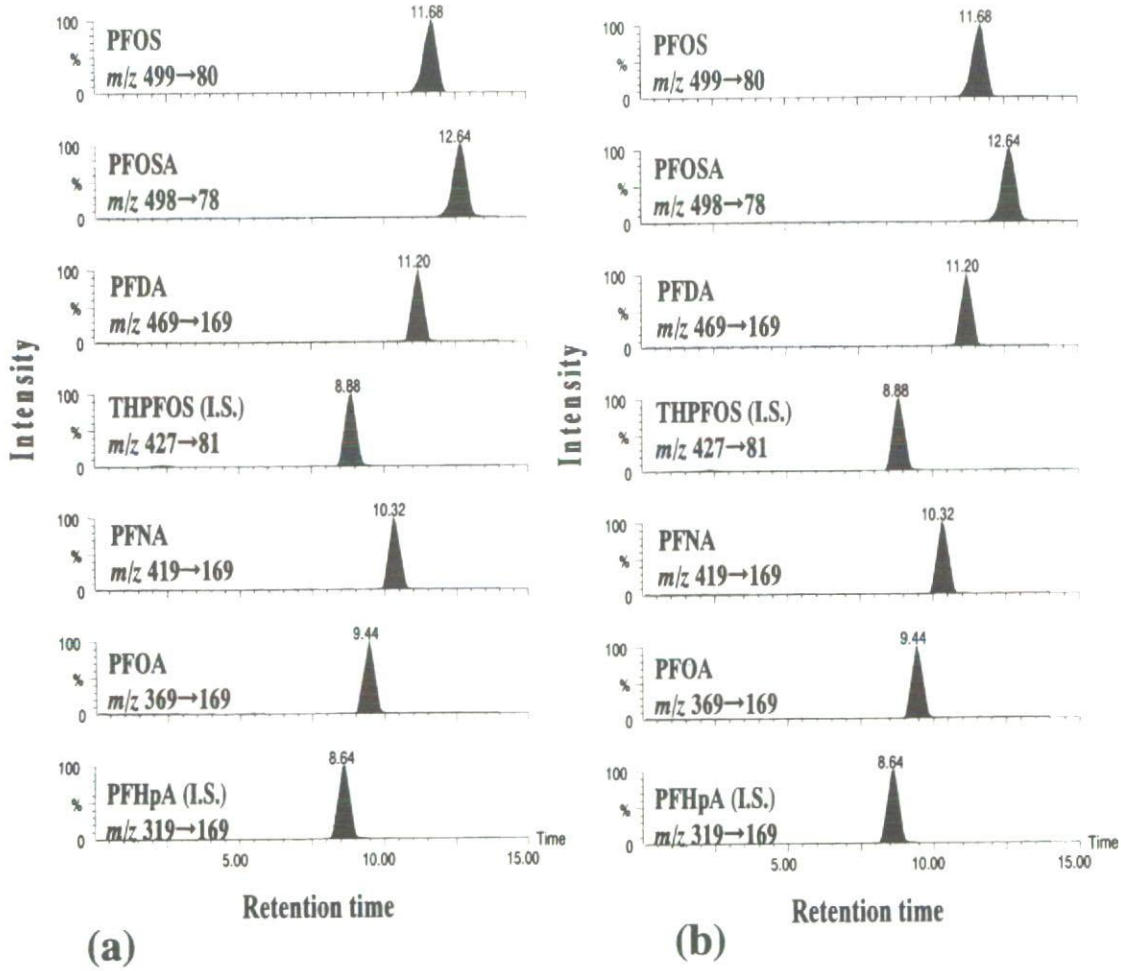

Fig. 7 MRM chromatograms of (a) a mixture of standards (PFOS, PFOSA, PFOA, PFNA, PFDA) and internal standards; (b) pooled human plasma with addition of 10 ng/ml PFCs

Table 2　Recovery levels of PFOS, PFOSA, PFOA, PFNA and PFDA in human plasma samples

Compound	Spiked amount/ ng ml^{-1}, human plasma sample	Average recovery, %	RSD, %
PFOS	5	99.3	3.0
	50	97.5	6.3
PFOSA	1	98.3	4.2
	10	105	4.2
PFOA	1	100	8.9
	10	97.3	4.8
PFNA	1	96.7	8.4
	10	94.7	3.1
PFDA	1	93.3	8.7
	10	103	4.7

$n = 6$

Table 3　Concentration of PFOS, PFOSA, PFOA, PFNA and PFDA in plasma samples from healthy volunteers

Volunteer	PFOS	PFOSA	PFOA	PFNA	PFDA
A (male)	5.6 ± 0.15	N.D.	1.7 ± 0.13	N.D.	N.D.
B (male)	17.7 ± 0.35	N.D.	2.8 ± 0.11	1.0 ± 0.05	N.D.
C (male)	21.3 ± 1.35	N.D.	4.6 ± 0.06	0.8 ± 0.05	N.D.
D (female)	2.1 ± 0.09	N.D.	0.7 ± 0.02	N.D.	N.D.
E (female)	10.4 ± 0.31	N.D.	2.4 ± 0.14	N.D.	N.D.
F (female)	15.1 ± 0.91	N.D.	1.9 ± 0.07	0.6 ± 0.02	N.D.

mean ± SD ng ml^{-1}, N.D. < 0.5 ng ml^{-1}, $n = 3$

定が可能となった．先に報告したカラムスイッチング-HPLC/MS法[18)19)]と本法を比較すると，測定装置にMS/MSを用いることでバックグラウンドの影響を軽減することができ，回収率が93.3%以上と向上した．また，分析カラムに50 mmのODSカラムを用いたことで，測定時間を15分に短縮することができた．再現性に関しては，前報では，オンライン固相抽出の溶離液に水/メタノール混液を用いていたが，今回，50 mM酢酸・酢酸アンモニウム緩衝液（pH = 4.7）/メタノール混液を用いたことで，保持時間のRSD（%）値が1.1%以下と良好な結果が得られた．以上のことから，本法は前報[18)19)]に比べて迅速かつ高い分析精度でPFCsの測定が可能となった．更に本法をヒト血しょう試料に応用したところ，PFOS，PFOA及びPFNAを検出することができた．今後，本法が多くのヒト血液試料の分析に用いられることにより，大規模な疫学研究等が実施され，PFOS及びPFOS関連化合物のリスク評価に資するものと期待される．

文　献

1) J. P. Giesy, K. Kannan: *Environ. Sci. Technol.*, **35**, 1339 (2001).
2) K. Kannan, S. Corsolini, J. Falandysz, G. Oehme, S. Focardi, J. P. Giesy: *Environ. Sci. Technol.*, **36**, 3210 (2002).
3) K. Kannan, J. Newsted, R. S. Halbrook, J. P. Giesy: *Environ. Sci. Technol.*, **36**, 2556 (2002).
4) K. J. Hansen, H. O. Johnson, J. S. Eldridge, J. L. Butenhoff, L. A. Disk: *Environ. Sci. Technol.*, **36**, 1681 (2002).
5) S. Taniyasu, K. Kannan, Y. Horii, N. Hanari, N. Yamashita: *Environ. Sci. Technol.*, **37**, 2634 (2003).
6) J. R. Thibodeaux, R. G. Hanson, J. M. Rogers, B. E. Grey, B. D. Barbee, J. H. Richards, J. L. Butenhoff, L. A. Stevenson, C. Lau: *Toxicol. Sci.*, **74**, 369 (2003).
7) C. Lau, J. R. Thibodeaux, R. G. Hanson, J. M. Rogers, B. E. Grey, M. E. Stanton, J. L. Butenhoff, L. A. Stevenson: *Toxicol. Sci.*, **74**, 382 (2003).
8) T. Ikeda, K. Aiba, K. Fukuda, M. Tanaka: *J. Biochem.*, **98**, 475 (1985).
9) A. K. Sohlenius, K. Andersson, J. DePierre: *J. Biochem.*, **285**, 779 (1992).
10) Y. Kawashima, N. Uy-Yu, H. Kozuka: *J. Biochem.*, **261**, 595 (1989).
11) X. Han, T. A. Show, R. A. Kemper, G. W. Jepson: *Chem. Res. Toxicol.*, **16**, 775 (2003).
12) X. Han, P. M. Hinderliter, T. A. Show, G. W. Jepson: *Drug. Chem. Toxicol.*, **27**, 341 (2004).
13) S. Taniyasu, K. Kannan, Y. Horii, N. Hanari, N. Yamashita: *Environ. Sci. Technol.*, **37**, 2634 (2003).
14) G. W. Olsen, K. J. Hansen, L. A. Stevenson, J. M. Burris, J. H. Mandel: *Environ. Sci. Technol.*, **37**, 888 (2003).
15) K. Kannan, S. Corsolini, J. Falandysz, G. Fillmann, K. S. Kumar, B. G. Loganathan, M. A. Mohd, J. Olivero, J. H. Yang, K. M. Aldous: *Environ. Sci. Technol.*, **38**, 4489 (2004).
16) Z. Kuklenyik, J. A. Reich, J. S. Tully, A. M. Calafat: *Environ. Sci. Technol.*, **38**, 3698 (2004).